THE JOURNAL OF PHYSICAL CHEMISTRY C

Article

Nanoparticle Multivalency Directed Shifting of Cellular Uptake Mechanism

Chumki Dalal, Arindam Saha, and Nikhil R. Jana

J. Phys. Chem. C, **Just Accepted Manuscript** • DOI: 10.1021/acs.jpcc.5b11059 • Publication Date (Web): 09 Mar 2016

Just Accepted

The Journal of Physical Chemistry C is published by the American Chemical Society.
1155 Sixteenth Street N.W., Washington, DC 20036

Nanoparticle Multivalency Directed Shifting of Cellular Uptake Mechanism

Chumki Dalal,[1] Arindam Saha*,[2] and Nikhil R. Jana*,[1]

[1]Centre for Advanced Materials, Indian Association for the Cultivation of Science, Kolkata-700032, India.

[2]Sensor and Actuator Division, CSIR-Central Glass and Ceramic Research Institute, Kolkata-700032, India

*Corresponding authors. E-mail: *camnrj@iacs.res.in* and *arindamsaha@cgcri.res.in*

ABSTRACT: Although nanoparticle multivalency is known to influence their biological labelling performance, the functional role of multivalency is largely unexplored. Here we show that folate receptor mediated cellular internalization mechanism of 35-50 nm nanoparticle shifts from caveolae- to clathrin-mediated endocytosis as the nanoparticle multivalency increases from 10 to 40 and results in the difference of their subcellular trafficking. We have synthesized folate functionalized multivalent quantum dot (QD) with varied average numbers of folate per QD between 10 to 110 [e.g. QD(folate)$_{10}$, QD(folate)$_{20}$, QD(folate)$_{40}$, QD(folate)$_{110}$] and investigated their uptake and localization into folate receptor over-expressed HeLa and KB cells. We found that uptake of QD(folate)$_{10}$ occurs predominantly via caveolae-mediated endocytosis and entirely trafficked to the perinuclear region. In contrast, uptake of QD(folate)$_{20}$ occurs via both caveolae- and chathrin-mediated endocytosis; uptake of QD(folate)$_{40}$ and QD(folate)$_{110}$ occurs predominantly via clathrin-mediated endocytosis and these three QDs localize predominantly at lysosome with restricted trafficking to perinuclear region. This work shows the functional role of multivalent interaction in cellular endocytosis and intracellular trafficking which can be exploited for subcellular targeting application.

INTRODUCTION

A variety of nanoparticle-based bioprobes are under development as alternative of molecular probes.[1-8] These nanoprobes are bright, stable and expected to provide better information of biological environment.[9-11] Common structure of nanoprobes have nanoparticle core, molecular/polymeric shell and covalently linked affinity biomolecule at their surface.[8] The typical number of biomolecule per nanoparticle varies between < 100 to few hundreds.[1-8,12-16] As a nanoprobe interacts with biological interface via affinity biomolecule, the nature of the interaction becomes multivalent and nanoprobe multivalency influences the labeling performance.[12-20] This multivalent property of nano and larger sized probes (10-100 times as compared to molecular probes) offers different ways of cellular uptake mechanism which are highly sensitive to nanoparticle size, shape and surface chemistry.[7] Literature study shows that most of the reported nanoprobes enter into cells via clathrin-mediated endocytosis and traffics to lysosome and raises substantial challenges in the development of subcellular nanoprobe.[7] In addition, currently available synthetic approaches are very limited in controlling the number of attached biomolecules per nanoparticle. Thus, the functional role of nanoprobe multivalency toward biological labeling performance and the possibility of subcellular targeting via controlling this multivalency is largely unexplored.

Multivalent and co-operative binding is common in biology that dictates the interaction involving biomolecules and biochemical processes.[21,22] A similar type of multivalent interaction has been observed in cell-nanoparticle interaction and exploited for efficient biolabeling and bioimaging application.[12-20] For example, cellular interaction and uptake of nanoparticle is shown to depend on the number of RGD peptide per nanoparticle with the maximum for 20 RGD,[13] number of HER2 per nanoparticle with the maximum for 11-23 HER2,[19] number of TAT peptide per nanoparticle,[12] number of oligonucleotide per nanoparticle[14] and number of folate per nanoparticle.[18,20] In addition, it is also observed that

monovalency of nanoprobes reduces their clustering on cell surface during the internalization processes.[15]

Most of the reported nanobioconjugate has an uncontrolled number of biomolecules and it is often not clear if the observed difference in cellular interaction with nanoprobes is due to the nanoparticle itself or to the chemical functional group on the surface, or due to attached biomolecule(s).[7,8] In addition the uptake mechanism of nanobioconjugate often differs from respective molecular probes and it is not clear if the nanoparticle or biomolecule is responsible for this difference in uptake mechanism. For example, folate receptor-mediated uptake of molecular probe occurs via caveolae-mediated endocytosis[23-26] but nanoprobe uptake occurs via clathrin- or both clathrin- and caveolae-mediated endocytosis.[27-32] A similar type of change in uptake mechanism is also observed after nanoparticle is functionalized with peptide,[33,34] vitamin[35] and antibody.[36,37] Here we show that nanobioconjugate can switch the endocytosis uptake mechanism from one to another via changing their multivalency. We have shown that folate receptor-mediated cellular uptake mechanism of folate functionalized nanoparticle depends on the nanoparticle multivalency, i.e., the number of folate attached on nanoparticle surface. For the multivalency of < 10, the nanoprobe enters into cell via the caveolae-mediated endocytosis and is transported into perinuclear region – as commonly observed for molecular probes. As the multivalency becomes > 10, additional clathrin-mediated endocytosis is initiated and for multivalency > 40, clathrin-mediated endocytosis dominates. This shifting of endocytosis mechanism from caveolae- to clathrin- maximizes the lysosomal trafficking of nanoprobe. This finding explains earlier reports of dominant clathrin-mediated endocytosis of different nanoprobes and demonstrates the importance of fine tuning nanoparticle multivalency in controlling the receptor-mediated endocytosis and their efficient subcellular targeting.

EXPERIMENTAL SECTION

Materials. Cadmium oxide, tri-octyl phosphine, tri-octyl phosphine oxide, stearic acid, zinc stearate, sulfur powder, selenium powder, fluorescein-NHS, folic acid, N-hydroxy succinimide (NHS), di-cyclohexyl carbodimide, poly(ethylene glycol) methacrylate, 3-sulfopropyl methacrylate, N,N-methylenebis(acrylamide), chlorpromazine hydrochloride, genistein, amiloride hydrochloride, methyl-β-cyclodextrin and folate free RPMI-1640 culture medium were purchased from Sigma-Aldrich and used as received. Hoechst, lysotracker red were purchased from Life Technology.

Nanoprobe Synthesis. Hydrophobic CdSe/ZnS core-shell quantum dots (QD) with red emission were synthesized using reported method.[8] These QDs were then transformed into hydrophilic nanoparticles via polyacrylate coating by our reported method.[8] In brief, hydrophobic QD was dissolved in 10 mL igepal-cyclohexane reverse micelle solution and mixed with aqueous solution of acrylate monomers. We have used N-(3-aminopropyl)-methacrylamide hydrochloride that provide primary amine functional group, 3-sulfopropropyl methacrylate that provide anionic charge, poly (ethylene glycol) methacrylate that provide polyethyleneglycol functionality and bis [2-(methacryloyloxy) ethyl] phosphate that function as cross-linker. The optically clear solution was purged with nitrogen and mixed with tetramethyl ethylenediamine and aqueous solution of ammonium persulphate to initiate the polymerization. The reaction was continued for one hour and then ethanol was added to quench the reaction. Precipitated QD was washed with chloroform and ethanol and finally dispersed in double distilled water. This process produces polyacrylate coated QD of 30-40 nm hydrodynamic diameters and with ~ 125 average number of primary amine per QD.

Next, folate functionalized QD was synthesized via competitive bioconjugation method reported earlier.[20] In brief, polyacrylate coated QD was reacted with a mixture of NHS-folate and NHS-fluorescein with varying molar ratio. Under this condition two NHS

reagents competes for reaction with primary amines present on QD surface and the number of folate bound to QD would depends on mole of NHS-folate. The reaction was continued for overnight and finally the solution was dialyzed to remove unbound reagents. Following this approach the number of folate per QD has been varied between 10 to 110, and results are summarized in Table 1.

Estimation of Number of Folate per QD. Number of folic acid per QD was estimated by our reported method.[20] In brief, concentration of QD was measured by using molar extinction coefficient of QD. Next, folate functionalized QD samples were treated with HCl to dissolve the QD and neutralized by adding NaOH. Then concentration of folate and fluorescein were determined by measuring the fluorescence intensity of folate and fluorescein. Finally, number of folate per QD was calculated from the ratio of concentration of folate and the concentration of QD.

Cell Labeling Study. Human cervical cancer cell line HeLa and KB cells were used as positive folate receptor cells. Cells were cultured in folate free RPMI-1640 (Invitrogen) with 10% heat activated fetal bovine serum (FBS) and 1% penicillin streptomycin at 37 $^{\circ}$C and 5 % CO_2 atmosphere. Cells were cultured overnight in a 24-well plate with 500 μL medium and then 30 μL QD sample was added followed by 1-3 hrs incubation. Next, cells were washed with PBS buffer solution and washed cells were used for imaging study or further incubated with fresh medium for 1-24 hrs followed by imaging study. Control cell labeling experiments were performed by adding free folic acid (100 μg/mL) in culture medium and by incubating cells at 4 $^{\circ}$C.

Co-Localization Study. Cells were cultured in a 24 well plates for 24 hours in folate free RPMI medium. Cells were incubated with QD samples for 3 hrs for their uptake by cells. Next, cells were washed with PBS buffer and fresh medium was added and kept for the next

12 hrs. Next, cells were incubated with lysotracker red for 15 mins and washed cells were used for imaging study.

Endocytosis Inhibition Study. For the endocytosis mechanism study, cells were taken in folate free RPMI medium and incubated with an inhibitor of desired concentration for one hour. Next, 30 μL QD sample was added and mix was further incubated for 1-2 hrs. The cells were then washed with PBS buffer for two times to remove unbound QD from the cell surface and used for imaging. For quantitative measurement cells were treated with 100 μL trypsin-EDTA for 2 mins and detached cells were isolated by centrifuge. Finally, cells were dispersed in PBS buffer and used for Flow Cytometric, fluorescence and ICP measurements. Typically, 200 μL of QD labeled dispersed cells of 0.1-0.5 millions were used for these studies and for ICP measurements cells were digested in 10% suprapure (ICP grade) HNO_3 .

Instrumentation. UV-visible absorption spectral studies were carried out with a Shimadzu UV-2550 UV-visible spectrophotometer**.** The DLS size and zeta potential were measured by Malvern Nano ZS instrument. Transmission electron microscopic (TEM) study was carried out using FEI Tecnai G2 F20 microscope. Flow Cytometry was performed using BD Accuri C6 Flow Cytometer, fluorescence-based quantification was performed using Synergy Mx monochromator based multimode fluorescence microplate reader (BioTek) and ICP-based quantification was performed using Optima 2100DV inductively coupled plasma atomic emission spectroscopy (ICP-AES, Perkin Elmer). Fluorescence image of cells were captured by Olympus IX 81 microscope using image-pro plus version 7.0 software and Carl Zeiss Apotome Imager Z1 microscope.

RESULTS

Synthesis of Folate Functionalized Nanoparticle of Varied Multivalency. Folate functionalized nanoparticle with a varied number of folate per nanoparticle was synthesized using our reported method.[20] In first step hydrophobic quantum dot (QD) is transformed into polyacrylate coated QD with low number (typically ~125) of surface terminated primary amines. Polyacrylate shell of these QD is made of polyethylene glycol (PEG) and appropriate ratio of amines and sulfates so that non-specific interaction with cell is minimum and nanoparticle has insignificant uptake by HeLa/KB cells unless functionalized with folate.[20] Next, primary amines are reacted with N-hydroxysuccinamide (NHS) derivative of folic acid (NHS-folate) for the preparation of folate functionalized QD. The number of attached folate per QD was controlled between 10-110 via competitive bioconjugation method.[20] In brief, amine functionalized QD is reacted with mixture of NHS-folate and NHS-fluorescein with their varied molar ratio, where the number of folate attached to QD depends on the molar ratio of NHS-folate used. Next, excess reagents are removed by dialysis and number of folate per QD is determined by using the fluorescence property of QD, folate and fluorescein.[20] In particular, we have synthesized folate functionalized QD with variable multivalency such as $QD(folate)_{10}$, $QD(folate)_{20}$, $QD(folate)_{40}$ and $QD(folate)_{110}$.(Scheme 1) Characterization of these functional QDs is shown in Figure 1, Supporting Information, Table S1, Figure S1, S2 and details of their properties are summarized in Table 1. All these particles have QD core and polyacrylate shell with overall hydrodynamic size of 35-50 nm and anionic surface charge.

Nanoparticle Multivalency Effects in Cell Uptake Mechanism and Subcellular Trafficking of Nanoparticle. Next, we study the uptake of functional QD by folate receptor over-expressed HeLa and KB cells. Results are summarized in Figure 2-7, Table 1 and Supporting Information, Figure S3-S14. Three types of control experiments have been

performed to confirm the folate receptor based selective labelling. In the first control experiment labelling is performed using QD without folate functionalization. (see Supporting Information, Figure S3) Results show that QD cannot label HeLa and KB cells when they are not functionalized with folate. In second control experiment folate functionalized QD is used for the labelling of cells that do not have over-expressed folate receptors and results show that QD cannot label such cells.[20] In third control experiment no labelling of folate functionalized QD is observed in presence of free folic acid in the cell culture medium. (Supporting Information, Figure S4) These results confirm selective labelling and uptake of folate functionalized QD by cells having over expressed folate receptors. It is know that proteins from culture media may adsorb on the nanoparticle surfaces and thus cells may not see the folate functionalization.[38] In order to understand this issue we have measured the hydrodynamic size and surface charges of the folate functionalized nanoparticles in serum containing and serum free cell culture media. We found that there is no significant change in their hydrodynamic size and surface charges. (Supporting Information, Table S1 and Figure S1) In addition we have also studied uptake of QD(folate)$_{10}$ and QD(folate)$_{110}$ in serum free cell culture media. We have not seen any significant difference on their cell uptake. (Supporting Information, Figure S5) These results conclude that proteins have poor binding with QD surface and QD interacts with cell using folic acid. This result is expected as our nanoparticles are coated with polyethylene glycol (PEG) that is known to reduce the non-specific interactions.

Energy dependent internalization of these QDs has been confirmed by incubating the HeLa cells with folate functionalized nanoparticles at 4 $^{\circ}$C. Reduced cellular uptake confirms energy dependent endocytosis mechanism (Supporting Information, Figure S6) Mechanism of cellular uptake has been investigated using various inhibitors that are known to hinder different endocytosis mechanism. We have used chlorpromazine (CHP) that blocks clathrin-

mediated endocytosis, amiloride that block macropinocytosis, genistein (GEN) that block caveolae-mediated endocytosis and methyl-β-cyclodextrin (MBCD) that blocks lipid raft-mediated endocytosis. Typically, cells are taken in folate free culture medium, incubated with inhibitors of desired concentration for one hour followed by incubation with QD samples. (see Supporting Information, Table S2 for details). Next, labeling of QD is thoroughly investigated and quantified. Results clearly show that all the QD samples have high labeling and cell uptake in absence of any inhibitors. However, in presence of inhibitors they behave differently. Results of HeLa cells are shown in Figure 2, Figure 3 and Supporting Information Figure S7. Although amiloride and MBCD hardly affect labeling property of all the QD, CHP and GEN are observed to influence the QD labeling depending on multivalency. In particular GEN completely inhibits QD(folate)$_{10}$ uptake and significantly inhibits QD(folate)$_{20}$ uptake. In contrast CHP significantly inhibit uptake of QD(folate)$_{20}$, QD(folate)$_{40}$ and QD(folate)$_{110}$. However, uptake inhibition of QD(folate)$_{10}$ by CHP is very insignificant.

Inhibitor induced differential QD uptake has been quantified by three different approaches such as cadmium estimation via inductively coupled plasma atomic emission spectroscopy (ICP-AES), QD fluorescence measurement using fluorescence plate reader and QD fluorescence measurement using flow cytometry. Figure 3 summarizes the results of three methods in HeLa cells and they reasonably furnish similar conclusions and corroborate with fluorescence imaging results shown in Figure 2. All the results clearly show that QD(folate)$_{10}$ uptake is almost completely inhibited by GEN, slightly inhibited by CHP and other inhibitors are unable to hinder their uptake. In contrast, the uptake of QD(folate)$_{20}$ is predominantly inhibited by both GEN and CHP but amiloride/MBCD are unable to prevent their uptake. The uptake of QD(folate)$_{40}$ and QD(folate)$_{110}$ are inhibited significantly by CHP, only slightly inhibited by GEN and almost unaffected by amiloride/MBCD. These results clearly suggest that uptake of QD(folate)$_{10}$ occurs predominantly via caveolae-mediated

endocytosis but uptake of QD(folate)$_{40}$ and QD(folate)$_{110}$ occurs predominantly via clathrin-mediated endocytosis and uptake of QD(folate)$_{20}$ occurs via both clathrin- and caveolae-mediated endocytosis.

Similar type multivalency dependent QD uptake is also observed in KB cells. (Figure 4, Supporting Information, Figure S8) In this case we have used three additional inhibitors such as nystatin[25] which inhibits the caveolae mediated endocytosis, sucrose[27] which inhibits clathrin mediated endocytosis and cytochalasin-D[34] (cyto-D) which inhibits macropinocytosis. Cell imaging study shows that amiloride, cyto-D, and MBCD hardly affect labeling property of all QD but GEN and nystatin significantly inhibits QD(folate)$_{10}$ uptake and CHP and sucrose significantly inhibit QD(folate)$_{110}$ uptake. (Supporting Information, Figure S8) Flow cytometry based quantification study shows that QD(folate)$_{10}$ uptake is almost completely inhibited by GEN and nystatin, partially inhibited by MBCD but amiloride/CHP/cyto-D/sucrose is unable to hinder their uptake. (Figure 4) In contrast, the uptake of QD(folate)$_{110}$ is predominantly inhibited by CHP and sucrose, partially inhibited by GEN and amiloride/MBCD/cyto-D/nystatin is unable to prevent their uptake. These results suggest that KB cell also follow same trend as of HeLa cell, i.e. entry of lower valent QD(folate)$_{10}$ occurs predominantly via caveolae mediated endocytosis but entry of higher valent QD(folate)$_{110}$ occurs predominantly via clathrin-mediated endocytosis. In addition we have used mixture of two inhibitors (CHP and amiloride) and found no significant changes on their uptake. (Figure 4 and Supporting Information, Figure S8)

Another control experiment has been performed to investigate the uptake of QD(folate)$_{110}$ in presence of both endocytosis inhibitors CHP and GEN together. (Supporting Information, Figure S9) The result shows that uptake of QD(folate)$_{110}$ is totally inhibited in presence of CHP and GEN together. In contrast uptake of QD(folate)$_{110}$ is not completely inhibited in presence of CHP only. This result indicates that both clathrin- and caveolae-

mediated endocytosis are operative for QD(folate)$_{110}$ but clathrin-mediated endocytosis dominates in normal condition and once CHP is added to block the clathrin-mediated endocytosis, the caveolae-mediated endocytosis becomes operative.

We have also observed multivalency dependent subcellular localization of QD nanoprobe. (Figure 5) This study is performed by incubating QD samples with KB cells, followed by washing to remove unbound particles and observing the localization of endocytosized QD for next 24 hrs. It is observed that QD(folate)$_{10}$ is trafficked to perinuclear region and concentrate at one side of the nucleus. High magnification fluorescence images of nuclear probe and QD(folate)$_{10}$ labeled cells at different Z planes shows that QDs localizes at the same plane of the nucleus and merged image shows that QD(folate)$_{10}$ localizes at the perinuclear region. (Supporting Information, Figure S10 and Figure S11) In contrast all other QDs fail to localize at perinuclear region. Further colocalization study with lysotracker red suggests that QD(folate)$_{40}$ and QD(folate)$_{110}$ are predominantly trafficked to lysosome within 12 hrs. (Figure 6 and Supporting Information, Figure S12) High magnification fluorescence images of lysotracker red and QD(folate)$_{110}$ labeled cells also confirm that higher multivalent QDs are localized at lysosome. (Figure 6) Subcellular localization of QD(folate)$_{10}$ is followed at different time point via colocalization study with lysotracker red and results show that QD(folate)$_{10}$ never localize with lysotracker red before trafficking to perinuclear region.(Supporting Information, Figure S13) This might be linked to their caveolae-mediated endocytosis where caveosome never fuse with lysosome and viruses usually choose caveolae mediated endocytosis to escape their lysosomal degradation.[39-42]

Control subcellular localization experiment has also been studied in presence of endocytosis inhibitors that significantly inhibits the QD uptake. In particular it has been observed that the lysosomal trafficking of higher multivalent QD can be redirected to perinuclear trafficking if clathrin-mediated endocytosis is blocked by CHP. A representative

result is provided in Figure 7. It shows that usual lysosomal trafficking of QD(folate)$_{110}$ can be successfully redirected towards perinuclear region if their clathrin mediated uptake is blocked by CHP. This result further suggests that caveolae-mediated uptake is suppressed by clathrin-mediated uptake in a higher multivalent QD but it can be operative under appropriate condition.

It is known that the kinetics of clathrin- mediated endocytosis is very fast as compared to caveolae- mediated endocytosis. We have performed additional control experiments to investigate the uptake kinetics of different QD with respect to the multivalency dependent shifting of endocytosis mechanism. It is found that QD(folate)$_{110}$ has relatively faster uptake rate than QD(folate)$_{10}$. (Supporting Information, Figure S14) We found that uptake of QD(folate)$_{110}$ is higher than QD(folate)$_{10}$ in one hour incubation. We also found that QD(folate)$_{110}$ colocalize with lysotracker red within 12 hrs. In contrast QD(folate)$_{10}$ takes 24 hrs to localize at perinuclear region. This result suggests that faster kinetics of clathrin-mediated endocytosis can suppress the slower caveolae-mediated endocytosis, even if the latter is partially operative. This mechanism can also explain perinuclear targeting of all QD in presence of CHP that blocks clathrin-mediated endocytosis.

DISCUSSION

Nanoparticle based probes are emerging alternative of molecular probes.[1,4] However, development of subcellular imaging nanoprobes is very challenging. Here we have designed nanoprobe with controlled multivalency, typically in the range of 10-100 in order to investigate their influence on biolabeling performances. Currently available synthetic approaches have limitations in controlling this multivalency and most of the reported nanoprobe/nanobioconjugate has multivalency of few hundreds.[7,8] Here we show that cell uptake mechanism and subcellular trafficking depends on nanoparticle multivalency. In

particular we have shown that high multivalency leads to clathrin-mediated endocytosis and lysosomal trafficking of nanoprobe that restricts their subcellular targeting. In contrast, nanoprobe having lower multivalency (typically < 10) enters into cell via caveolae-mediated endocytosis and localized to perinuclear region without trafficking at lysosome. The transition between clathrin- and caveolae- occurs typically in the multivalency range of 10-40 and thus nanoprobe multivalency in this range need to be carefully investigated.

The observed nanoprobe multivalency dependent cell uptake mechanism has special significance for subcellular targeting applications. It is well known that nature of endocytosis dictates the trafficking mechanism and subcellular localization of foreign materials.[39,41] For example, caveolae- and lipid raft-mediated endocytosis traffics materials through caveosome with lower chances of degradation because of neutral pH of caveosome.[43,44] Thus caveolae- and lipid raft-mediated endocytosis leads to efficient perinuclear trafficking of material, particularly to nucleus, endoplasmic reticulum and Golgi apparatus.[40,43] In contrast, clathrin-mediated endocytosis traffics the material to acidic endosomal/lysosomal compartments. In drug or gene delivery approach it is preferable that the nanoparticle does not traffic to lysosome where they can be degraded.[43,45,46] Thus preferential caveolae- and lipid raft-mediated endocytosis over clathrin-mediated endocytosis have enormous importance. However, this type of specific endocytosis remains a challenging issue and in reality clathrin-mediated endocytosis becomes most dominating pathway for nanoparticle, inhibiting their subcellular targeting.[47-53] Here we show that lowering of nanoparticle multivalency greatly enhances their subcellular targeting performance with minimum lysosomal trapping via modified uptake mechanism.

Presented results are based on enodocytosis of folic acid functionalized nanoparticle by folate receptor. Folate receptor is over-expressed in several types of cancer cells.[54] It is a GPI linked anchor protein that diffusely distributes on cell membrane and concentrate in

small flask shaped membrane invagination called caveolae.[26] The folate receptor is colocalized with caveolin which is an integral part of caveloae. It is known that clustering of GPI-anchored proteins regulate their sequestration in caveolae and promotes caveolae-mediated endocytosis. So, high concentration of folate bound receptors in caveolae is required for folate transport.[55] Thus it is expected that folate receptor mediated uptake of nanoparticle is linked to the clustering property of folate receptors by nanoparticle.[26] In particular nanoparticle with varied multivalency can induce different extent of clustering of folate receptor and thus expected to modulate the endocytosis mechanism. Similar type of nanoparticle multivalency directed interaction is expected for nanoparticle functionalized with RGD peptide,[13] HER2,[19] TAT peptide[12] and oligonucleotide.[14]

Based on our result a mechanism is proposed to explain the role of nanoparticle multivalency in dictating the folate receptor-mediated cell uptake mechanism and in controlling the caveolae- vs clathrin-mediated endocytosis. (Scheme 2) Low multivalency (typically < 10) offers modular interaction of nanoparticle with cell surface receptors and directs the nanoprobe toward the caveolae. This event leads to the clustering of folate receptors followed by caveolae-mediated endocytosis. In contrast high multivalency (typically > 20) of nanoparticle can cause receptors to cluster on the cell surface via cross-linking.[26] Stronger binding of nanoprobe with cell surface via multiple receptors reduces the receptor mobility[15] and restricts nanoparticle localization at a fixed position of membrane and initiates additional signaling pathway for clathrin-mediated endocytosis. The faster kinetic of clathrin-mediated endocytosis over caveloae-mediated endocytosis leads the domination of clathrin-mediated endocytosis. When CHP is used to block the clathrin-mediated endocytosis (via binding with clathrin protein) the suppressed caveolae-mediated endocytosis becomes operative again.

Proposed mechanism can explain anomalies observed in folate receptor mediated endocytosis. Earlier work shows that uptake of folate functionalized protein, polymer, micelle and nanoparticle occurs by cavevolae- or clathrin-mediated endocytosis. For example, folate functionalized BSA/dextran (with 1-3 folate per polymer)[23,25] or liposome (with 365 folate per particle) enter into folate over-expressed KB cell via caveolae mediated endocytosis.[24] In contrast, folate functionalized silica particle and carbon nanotube (with uncontrolled number of folate per particle) enter into KB and HeLa cell via clathrin mediated endocytosis.[27,28] Folate functionalized polymer micelle enter into HeLa/KB/MCF-7 cell via both clathrin and caveolae mediated endocytosis.[30-32] There is also reports on change in uptake mechanism depending on particle size[30] or folate density,[32] surface chemistry,[27] role of folate multivalency on rate of endocytosis[56] and role of special arrangement of folate on *in vivo* targeting efficiency.[57]

Here we show the effect of folate multivalency on folate receptor mediated endocytosis mechanism and subcellular trafficking. In particular the proposed mechanism can explain the clathrin-mediated endocytosis often observed by folate functionalized nanoparticle. Proposed mechanism shows that higher multivalency and faster kinetics of clathrin-mediated endocytosis can induce preferential clathrin-mediate endocytosis. As commonly used nanoparticles have high multivalency, they often mask the caveolae-mediated endocytosis of folate functionalized nanoparticle.

CONCLUSION

We have shown that cell uptake mechanism of nanoparticle can be controlled by changing their multivalency, typically between 10-40. We have synthesized folate functionalized QD nanoprobe with varied multivalency and found that folate receptor mediated cellular internalization mechanism of QD shifts from caveolae- to clathrin-mediated

endocytosis, as the nanoparticle multivalency increases from 10 to 40. While caveolae-mediated uptake traffics nanoprobe into perinuclear region, chathrin-mediated endocytosis traffics them to lysosome. This work shows the importance of lower multivalency (typically < 10) of nanoparticle for efficient subcellular targeting and established the functional role of multivalent interaction in cellular endocytosis. Further study should be directed to prepare appropriate nanobioconjugate with lower multivalency for efficient subcellular targeting.

ASSOCIATED CONTENT

Supporting Information Available: Conditions used for labeling experiments, characterization details of nanoprobe, control labeling experiments and additional labeling data. This material is available free of charge via the Internet at http://pubs.acs.org.

Notes

The authors declare no competing financial interests.

Acknowledgement

The authors acknowledge DST, government of India for financial assistance. (No. SB/S1/IC-13/2013) C. D. acknowledges CSIR, India for research fellowship. A.S. acknowledges CSIR-India for Nehru postdoctoral fellowship.

REFERENCES

(1) Bruchez, M. J.; Moronne, M.; Gin, P.; Weiss, S.; Alivisatos, A. P. Semiconductor Nanocrystals as Fluorescent Biological Labels. *Science* **1998**, *281*, 2013−2016.

(2) Michalet, X.; Pinaud, F. F.; Bentolila, L. A.; Tsay, J. M.; Doose, S.; Li, J. J.; Sundaresan, G.; Wu, A. M.; Gambhir, S. S.; Weiss, S. Quantum Dots for Live Cells, in Vivo Imaging, and Diagnostics. *Science* **2005**, *307*, 538−544.

(3) Medintz, I. L.; Uyeda, H. T.; Goldman, E. R.; Mattoussi, H. Quantum Dot Bioconjugates for Imaging, Labelling and Sensing. *Nat. Mater.* **2005**, *4*, 435−446.

(4) Genger, U. R.; Grabolle, M.; Jaricot, S. C.; Nitschke, R.; Nann, T. Quantum Dots versus Organic Dyes as Fluorescent Labels. *Nat. Methods* **2008**, *5*, 763−775.

(5) Murphy, C. J.; Gole, A. M.; Stone, J. W.; Sisco, P. N.; Alkilany, A. M.; Goldsmith, E. C.; Baxter, S. C. Gold Nanoparticles in Biology: Beyond Toxicity to Cellular Imaging. *Acc. Chem. Res.* **2008**, *41*, 1721−1730.

(6) Ling, D.; Lee, N.; Hyeon, T. Chemical Synthesis and Assembly of Uniformly Sized Iron Oxide Nanoparticles for Medical Applications. *Acc. Chem. Res.* **2015**, *48*, 1276−1285.

(7) Sapsford, K. E.; Algar, W. R.; Berti, L.; Gemmill, K. B.; Casey, B. J.; Oh, E.; Stewart, M. H.; Medintz, I. L. Functionalizing Nanoparticles with Biological Molecules: Developing Chemistries that Facilitate Nanotechnology. *Chem. Rev.* **2013**, *113,* 1904−2074.

(8) Basiruddin, SK; Saha, A.; Pradhan, N.; Jana, N. R. Advances in Coating Chemistry in Deriving Soluble Functional Nanoparticle. *J. Phys. Chem. C* **2010**, *114*, 11009−11017.

(9) Dahan, M.; Lévi, S.; Luccardini, C.; Rostaing, P.; Riveau, B.; Triller, A. Diffusion Dynamics of Glycine Receptors Revealed by Single-Quantum Dot Tracking. *Science* **2003**, *302*, 442−445.

(10) Courty, S.; Luccardini, C.; Bellaiche, Y.; Cappello, G.; Dahan, M. Tracking Individual Kinesin Motors in Living Cells Using Single Quantum-Dot Imaging. *Nano Lett.* **2006**, *6*, 1491−1495.

(11) Zhang, R.; Rothenberg, E.; Fruhwirth, G.; Simonson, P. D.; Ye, F.; Golding, I.; Ng, T.; Lopes, W.; Selvin, P. R. Two-Photon 3D FIONA of Individual Quantum Dots in an Aqueous Environment. *Nano Lett.* **2011**, *11,* 4074−4078.

(12) Zhao, M.; Kircher, M. F.; Josephson, L.; Weissleder, R. Differential Conjugation of Tat Peptide to Superparamagnetic Nanoparticles and Its Effect on Cellular Uptake. *Bioconjugate Chem.* **2002**, *13*, 840−844.

(13) Montet, X.; Funovics, M.; Montet-Abou, K.; Weissleder, R.; Josephson, L. Multivalent Effects of RGD Peptides Obtained by Nanoparticle Display. *J. Med. Chem.* **2006,** *49*, 6087−6093.

(14) Giljohann, D. A.; Seferos, D. S.; Patel, P. C.; Millstone, J. E.; Rosi, N. L.; Mirkin, C. A. Oligonucleotide Loading Determines Cellular Uptake of DNA-Modified Gold Nanoparticles. *Nano Lett.* **2007**, *7*, 3818−3821.

(15) Howarth, M.; Liu, W.; Puthenveetil, S.; Zheng, Y.; Marshall, L. F.; Schmidt, M. M.; Wittrup, K. D.; Bawendi, M. G.; Ting, A. Y. Monovalent, Reduced-size Quantum Dots for Imaging Receptors on Living Cells. *Nat. Methods* **2008**, *5*, 397−399.

(16) Massich, M. D.; Giljohann, D. A.; Schmucker, A. L.; Patel, P. C.; Mirkin, C. A. Cellular Response of Polyvalent Oligonucleotide−Gold Nanoparticle Conjugates. *ACS Nano* **2010**, *10*, 5641−5646.

(17) Zhang, X. Q.; Xu, X. Y.; Lam, R.; Giljohann, D.; Ho, D.; Mirkin, C. A. Strategy for Increasing Drug Solubility and Efficacy through Covalent Attachment to Polyvalent DNA–Nanoparticle Conjugates. *ACS Nano* **2011**, *5*, 6962−6970.

(18) Moradi, E.; Vllasaliu, D.; Garnett, M.; Falcone, F.; Stolnik, S. Ligand Density and Clustering Effects on Endocytosis of Folate Modified Nanoparticles. *RSC Adv.* **2012**, *2*, 3025−3033.

(19) Elias, D. R.; Poloukhtine, A.; Popik, V.; Tsourkas, A. Effect of Ligand Density, Receptor Density, and Nanoparticle Size on Cell Targeting. *Nanomed. Nanotechnol. Biol. Med.* **2013**, *9*, 194−201.

(20) Saha, A.; Basiruddin, S. K.; Maity, A. R.; Jana, N. R. Synthesis of Nanobioconjugates with a Controlled Average Number of Biomolecules between 1 and 100 per Nanoparticle and Observation of Multivalency Dependent Interaction with Proteins and Cells. *Langmuir* **2013**, *29*, 13917−13924.

(21) Mammen, M.; Choi, S. K.; Whitesides, G. M. Polyvalent Interactions in Biological Systems: Implications for Design and Use of Multivalent Ligands and Inhibitors. *Angew. Chem. Int. Ed.* **1998**, *37*, 2754−2794.

(22) Kiessling, L. L.; Gestwicki, J. E.; Strong, L. E. Synthetic Multivalent Ligands in the Exploration of Cell-Surface Interactions. *Curr. Opin. Chem. Biol.* **2000**, *4*, 696−703.

(23) Turek, J. J.; Leamon, C. P.; Low, P. S. Endocytosis of Folate-Protein Conjugates: Ultrastructural Localization in KB Cells. *J. Cell. Sci.* **1993**, *106*, 423−430.

(24) Lee, R. J.; Low, P. S. Delivery of Liposomes into Cultured KB Cells via Folate Receptor-Mediated Endocytosis. *J. Biol. Chem.* **1994**, *269*, 3198−3204.

(25) Lee, R. J.; Low, P. S Measurement of Endosome pH Following Folate Receptor-Mediated Endocytosis. *Biochimica et Biophysica Acta-Mol. Cell Res.* **1996**, *1312*, 237−242.

(26) Sabharanjak, S.; Mayor, S. *Folate Receptor Endocytosis and Trafficking.* Adv. Drug Delivery Rev. **2004**, 56, 1099−1109.

(27) Slowing, I.; Trewyn, B. G.; Lin, V. S. Y. Effect of Surface Functionalization of MCM-41-Type Mesoporous Silica Nanoparticles on the Endocytosis by Human Cancer Cells. *J. Am. Chem. Soc.* **2006**, *128*, 14792−14793.

(28) Yang, H.; Lou, C.; Xu, M.; Wu, C.; Miyoshi, H.; Liu, Y. Investigation of Folate-Conjugated Fluorescent Silica Nanoparticles for Targeting Delivery to Folate Receptor-Positive Tumors and Their Internalization Mechanism. *Int. J. Nanomedicine* **2011**, *6*, 2023−2032.

(29) Niu, L.; Meng, L.; Lu, Q. Folate-Conjugated PEG on Single Walled Carbon Nanotubes for Targeting Delivery of Doxorubicin to Cancer Cells. *Macromol. Biosci.* **2013**, *13*, 735−744.

(30) Suen, W. L. L.; Chau, Y. Size-Dependent Internalisation of Folate-Decorated Nanoparticles via the Pathways of Clathrin and Caveolae-Mediated Endocytosis in ARPE-19 Cells. *J. Pharm. Pharmacol.* **2013**, *66*, 564−573.

(31) Li, Y. L.; Cuong, N. V.; Hsieh, M. F. Endocytosis Pathways of the Folate Tethered Star-Shaped PEG-PCL Micelles in Cancer Cell Lines. *Polymers* **2014**, *6*, 634−650.

(32) Cao, D.; Tian, S.; Huang, H.; Chen, J.; Pan, S. Divalent Folate Modification on PEG: An Effective Strategy for Improving the Cellular Uptake and Targetability of PEGylated Polyamidoamine–Polyethylenimine Copolymer. *Mol. Pharmaceutics* **2015**, *12*, 240−252.

(33) Fittipaldi, A.; Ferrari, A.; Zoppe, M.; Arcangeli, C.; Pellegrini, V.; Beltram, F.; Giacca, M. Cell Membrane Lipid Rafts Mediate Caveolar Endocytosis of HIV-1 Tat Fusion Proteins. *J. Biol. Chem*. **2003**, *278*, 34141−34149.

(34) Ruan, G.; Agarwal, A.; Marcus, A. I.; Nie, S. Imaging and Tracking of Tat Peptide-Conjugated Quantum Dots in Living Cells: New Insights into Nanoparticle Uptake, Intracellular Transport, and Vesicle Shedding. *J. Am. Chem. Soc.* **2007**, *129*, 14759−14766.

(35) Fowler, R.; Vllasaliu, D.; Trillo, F. F.; Garnett, M.; Alexander, C.; Horsley, H.; Smith, B.; Whitcombe, I.; Eaton, M.; Stolnik, S. Nanoparticle Transport in Epithelial Cells: Pathway Switching through Bioconjugation. *Small* **2013**, *9*, 3282−3294.

(36) Bhattacharyya, S.; Bhattacharya, R.; Curley, S.; McNiven, M. A. Mukherjee, P. Nanoconjugation Modulates the Trafficking and Mechanism of Antibody Induced Receptor Endocytosis. *Proc. Natl. Acad. Sci. USA*, **2010,** *107*, 14541−14546.

(37) Gao, H.; Yang, Z.; Zhang, S.; Cao, S.; Shen, S.; Pang, Z; Jiang, X. Ligand Modified Nanoparticles Increases Cell Uptake, Alters Endocytosis and Elevates Glioma Distribution and Iinternalization. *Sci. Rep.* **2013**, *3*, 2534.

(38) Mahmoudi, M.; Lynch, I.; Ejtehadi, M. R.; Monopoli, M. P.; Bombelli, F. B.; Laurent, S. Protein−Nanoparticle Interactions: Opportunities and Challenges. *Chem. Rev.* **2011**, *111*, 5610−5637.

(39) Mayor, S.; Pagano, R. E. Pathways of Clathrin-Independent Endocytosis. *Nat. Rev. Mol. Cell Bio.* **2007**, *8,* 603−612.

(40) Chakraborty, A.; Jana, N. R. Clathrin to Lipid Raft-Endocytosis via Controlled Surface Chemistry and Efficient Perinuclear Targeting of Nanoparticle. *J. Phys. Chem. Lett.* **2015**, *6*, 3688−3697.

(41) Ohannes, L.; Parton, R. G.; Bassereau, P.; Mayor, S. Building Endocytic Pits without Clathrin. *Nat. Rev. Mol. Cell Biol.* **2015**, *16*, 311−321.

(42) Orlandi, P. A.; Fishman, P. H. Filipin-dependent Inhibition of Cholera Toxin: Evidence for Toxin Internalization and Activation through Caveolae-like Domains. *J. Cell Biol.* **1998,** *141*, 905−915.

(43) Rejman, J.; Bragonzi, A.; Conese, M. Role of Clathrin- and Caveolae-Mediated Endocytosis in Gene Transfer Mediated by Lipo- and Polyplexes. *Mol. Ther.* **2005**, *12*, 468−474.

(44) Lee, J. H.; Twomey, M.; Machado, C.; Gomez, G.; Doshi, M.; Gesquiere, A. J.; Moon, J. H. Caveolae-Mediated Endocytosis of Conjugated Polymer Nanoparticles. *Macromol. Biosci.* **2013**, *13*, 913−920.

(45) Pelkmans, L.; Helenius, A. Endocytosis via Caveolae. *Traffic* **2002**, *3*, 311−320.

(46) Khalil, I. A.; Kogure, K.; Akita, H.; Harashima, H. Uptake Pathways and Subsequent Intracellular Trafficking in Nonviral Gene Delivery. *Pharmacol. Rev*. **2006**, *58*, 32−45.

(47) Chithrani, B. D.; Chan, W. C. W. Elucidating the Mechanism of Cellular Uptake and Removal of Protein-Coated Gold Nanoparticles of Different Sizes and Shapes. *Nano Lett.* **2007**, *7*, 1542−1550.

(48) Faklaris, O.; Joshi, V.; Irinopoulou, T.; Tauc, P.; Sennour, M.; Girard, H.; Gesset, C.; Arnault, J. C.; Thorel, A.; Boudou, J. P.; et al. Photoluminescent Diamond Nanoparticles for Cell Labeling: Study of the Uptake Mechanism in Mammalian Cells. *ACS Nano* **2009**, *3*, 3955−3962.

(49) Anas, A.; Okuda, T.; Kawashima, N.; Nakayama, K.; Itoh, T.; Ishikawa, M.; Biju, V. Clathrin-Mediated Endocytosis of Quantum Dot−Peptide Conjugates in Living Cells. *ACS Nano* **2009**, *3*, 2419−2429.

(50) Jiang, X. E.; Rocker, C.; Hafner, M.; Brandholt, S.; Dorlich, R. M.; Nienhaus, G. U. Endo- and Exocytosis of Zwitterionic Quantum Dot Nanoparticles by Live HeLa Cells. *ACS Nano* **2010**, *4*, 6787−6797.

(51) Jin, J. F.; Gu, Y. J.; Man, C. W. Y.; Cheng, J. P.; Xu, Z. H.; Zhang, Y.; Wang, H. S.; Lee, V. H. Y.; Cheng, S. H.; Wong, W. T. Polymer-Coated $NaYF_4$:Yb^{3+}, Er^{3+} Upconversion Nanoparticles for Charge-Dependent Cellular Imaging. ACS *Nano* **2011**, *5*, 7838−7847.

(52) Yang, L. X.; Shang, L.; Nienhaus, G. U. Mechanistic Aspects of Fluorescent Gold Nanocluster Internalization by Live HeLa Cells. *Nanoscale* **2013**, *5*, 1537−1543.

(53) Suresh, D.; Zambre, A.; Chanda, N.; Hoffman, T. J.; Smith, C. J.; Robertson, J. D.; Kannan, R. Bombesin Peptide Conjugated Gold Nanocages Internalize via Clathrin Mediated Endocytosis. *Bioconjugate Chem.* **2014**, *25*, 1565−1579.

(54) Vlahov, I. R.; Leamon, C. P. Engineering Folate–Drug Conjugates to Target Cancer: From Chemistry to Clinic. *Bioconjugate Chem.* **2012**, *23*, 1357−1369.

(55) Mayor, S.; Rothberg, K. G.; Maxfield, F. R. Sequestration of GPI-Anchored Proteins in Caveolae Triggered by Cross-Linking. *Science* **1994**, *264*, 1948–1951.

(56) Bandara, N. A.; Hansen, M. J.; Low, P. S. Effect of Receptor Occupancy on Folate Receptor Internalization. *Mol. Pharmaceutics* **2014**, *11*, 1007−1013.

(57) Poon, Z.; Chen, S.; Engler, A. C.; Lee, H.; Atas, E.; Maltzahn, G. V.; Bhatia, S. N.; Hammond, P. T. Ligand-Clustered "Patchy" Nanoparticles for Modulated Cellular Uptake and in vivo Tumor Targeting. *Angew. Chem. Int. Ed.* **2010**, *49*, 7266−7270.

Table 1: Composition, Property, Uptake Mechanism and Sub-Cellular Localization of Nanobioconjugates Used in this Study

NHS-folate (mole%)	Number of folate/QD	DLS size (nm)	Charge (mV)	Abbreviation	Cell uptake pathway	Sub-cellular localization
5	10±4	~35-40	-20	$QD(folate)_{10}$	caveolae	perinuclear region
18	20±5	~40-45	-20	$QD(folate)_{20}$	caveolae and clathrin	perinuclear region and lysosome
25	40±7	~45-50	-17	$QD(folate)_{40}$	clathrin	lysosome
95	110±10	~45-50	-14	$QD(folate)_{110}$	clathrin	lysosome

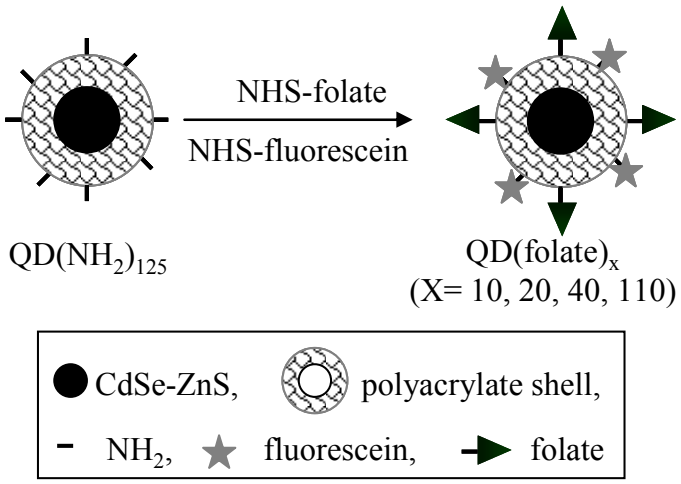

Scheme 1. Synthetic approach for the preparation of folate functionalized quantum dot (QD). Polyacrylate coated QD with ~125 primary amine per QD is reacted with mixture of NHS-folate and NHS-fluorescein of varied molar ratio for the preparation of $QD(folate)_{10}$, $QD(folate)_{20}$, $QD(folate)_{40}$ and $QD(folate)_{110}$.

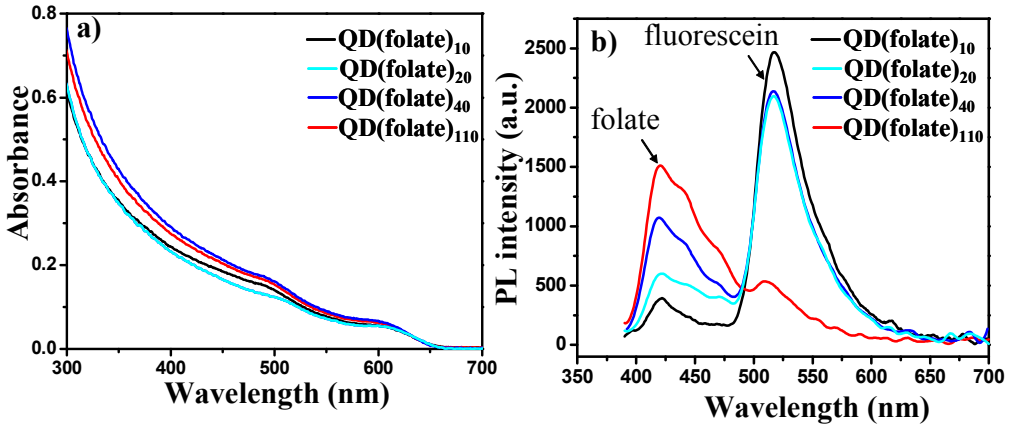

Figure 1. Absorption (a) and emission spectra (b) of QD samples used in this study. Concentrations of QD are normalized by maintaining same absorbance at 590 nm and emission spectra are obtained after dissolving QD by HCl addition followed by neutralizing with NaOH. Variation of folate and fluorescein are evident from the change of emission band intensity of folate/fluorescein.

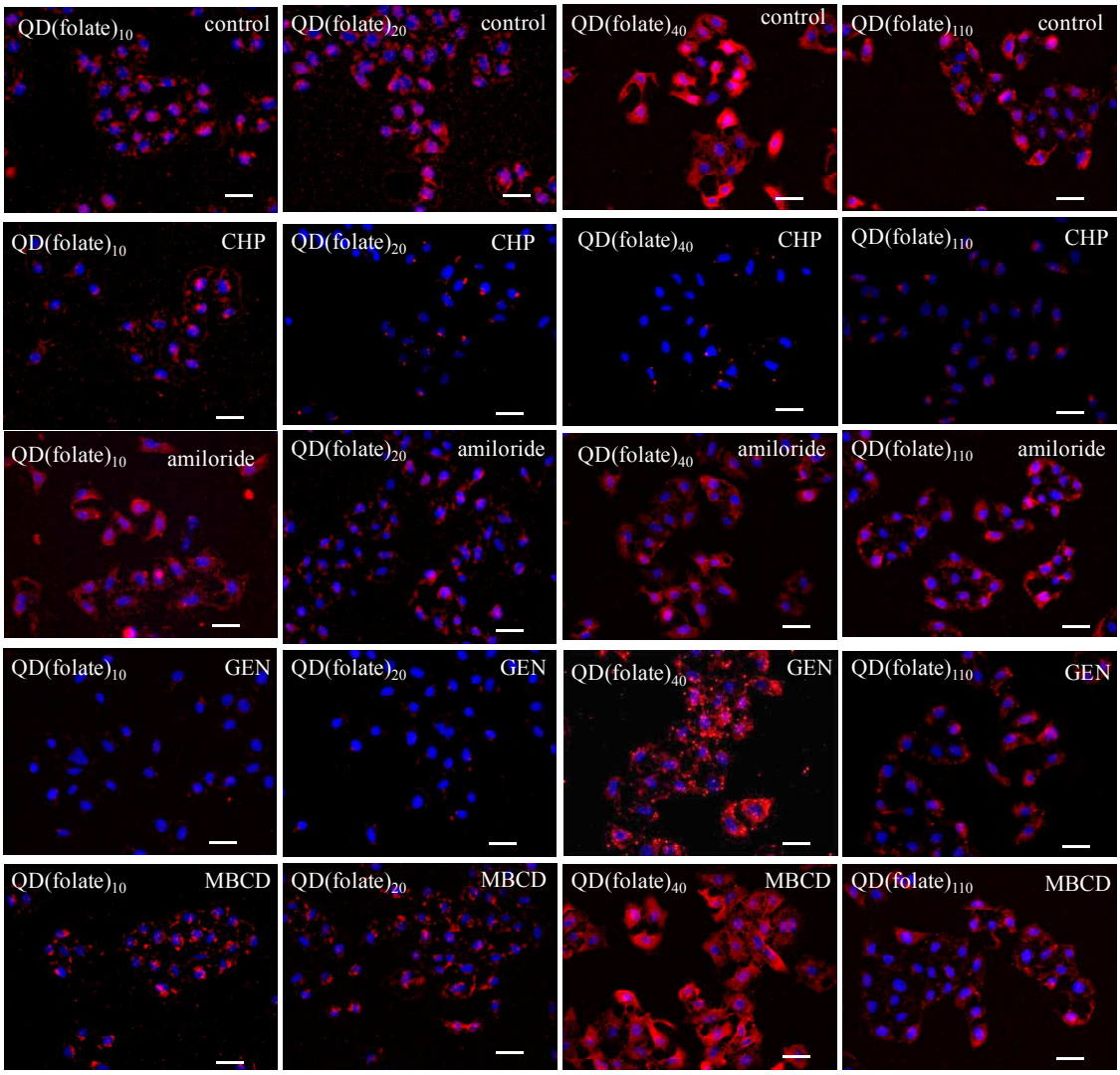

Figure 2. Fluorescence image of HeLa cells labelled with $QD(folate)_{10}$, $QD(folate)_{20}$, $QD(folate)_{40}$ and $QD(folate)_{110}$ in presence of different endocytosis inhibitors. Red color corresponds to QD and blue color corresponds to nuclear probe. Typically, cells are incubated with inhibitors followed by incubation with QD samples and then washed cells are imaged under fluorescence microscope. Images show that $QD(folate)_{10}$ uptake is predominantly inhibited by GEN only, $QD(folate)_{20}$ uptake is inhibited by both GEN and CHP but $QD(folate)_{40}$ and $QD(folate)_{110}$ uptake is significantly inhibited only by CHP. Scale bar represents 50 μm.

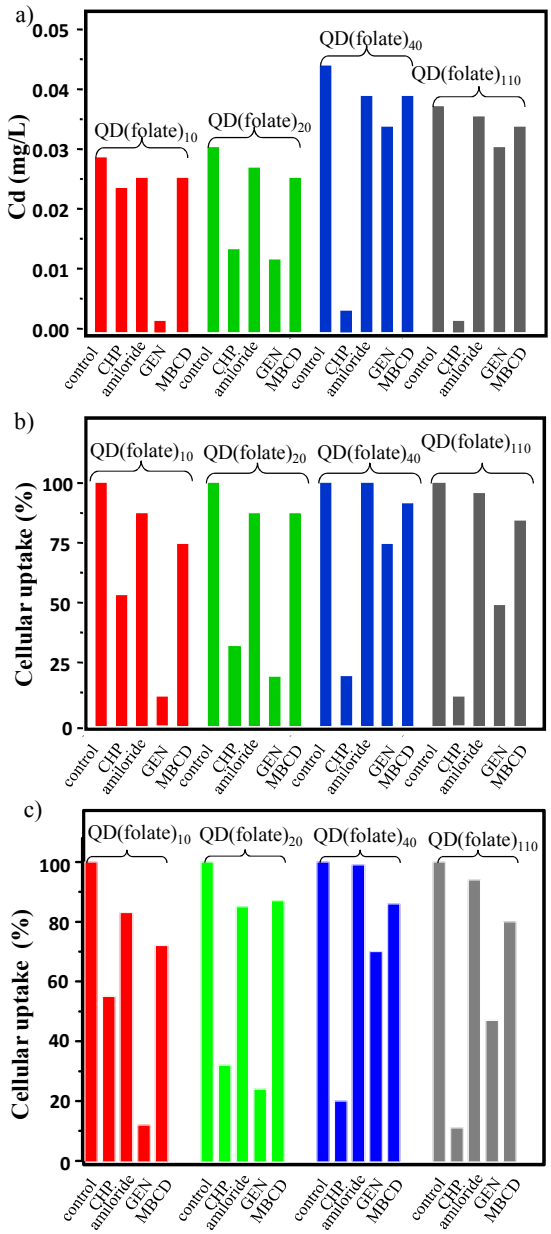

Figure 3. Quantitative estimation of QD uptake in HeLa cells in presence of different endocytosis inhibitors, using cadmium estimation via ICP (a), QD fluorescence measurement using flow cytometer (b) and QD fluorescence measurement using fluorescence plate reader (c). Typically, cells are incubated with inhibitors followed by incubation with different QD samples and then washed cells are used for quantifications. Three methods clearly show that QD(folate)$_{10}$ uptake is inhibited by GEN, QD(folate)$_{20}$ uptake is inhibited by both GEN and CHP but uptake of QD(folate)$_{40}$ and QD(folate)$_{110}$ is inhibited by CHP.

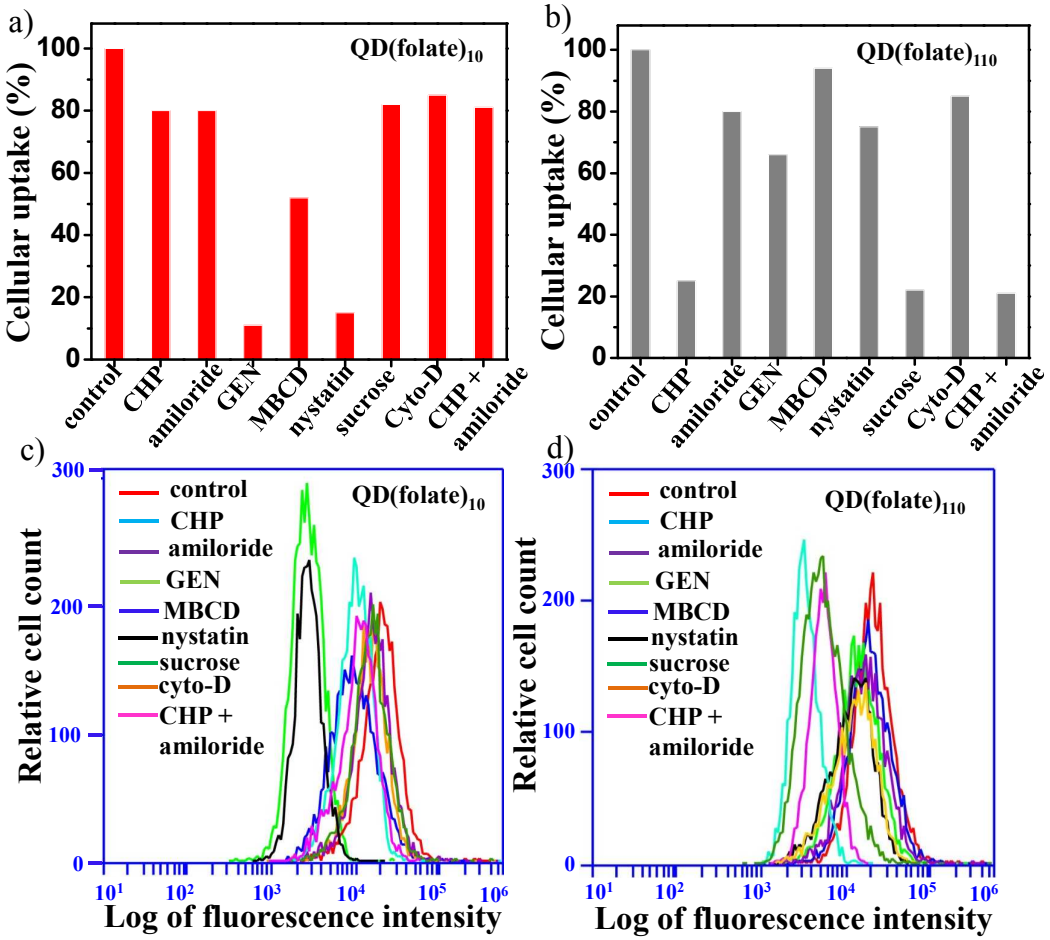

Figure 4. Flow cytometry based quantitative analysis of uptake of $QD(folate)_{10}$ (a,c) and $QD(folate)_{110}$ (b,d) in KB cells in presence of different endocytosis inhibitors. Result shows that $QD(folate)_{10}$ uptake is primarily inhibited by GEN and nystatin but uptake of $QD(folate)_{110}$ is primarily inhibited by CHP and sucrose.

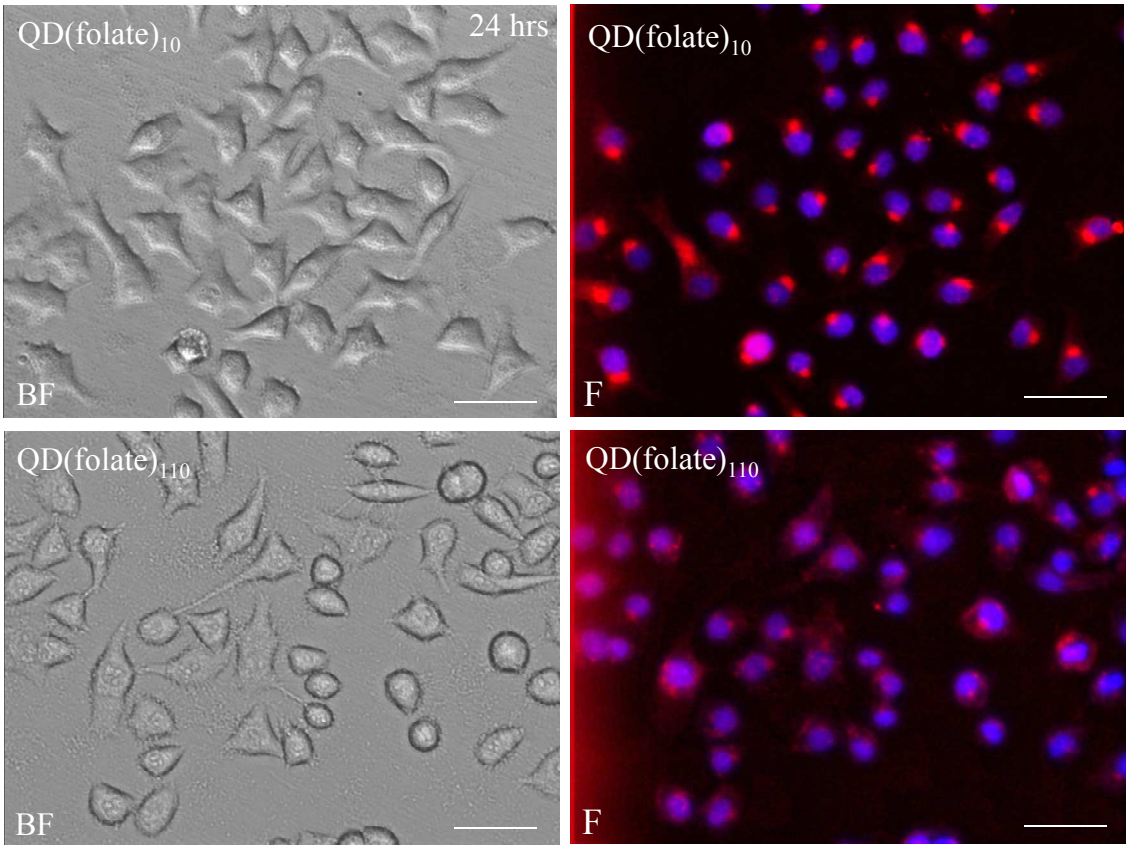

Figure 5. Subcellular localization of $QD(folate)_{10}$ and $QD(folate)_{110}$ in KB cells, showing that lowering of multivalency enhances the perinuclear targeting performance. QDs are incubated with cells for 3 hrs and washed cells are mixed with fresh culture medium for another 24 hrs before imaging under bright field (BF) or fluorescence (F) mode. Red color corresponds to QD and blue color corresponds to nuclear probe. Scale bar represents 50 μm.

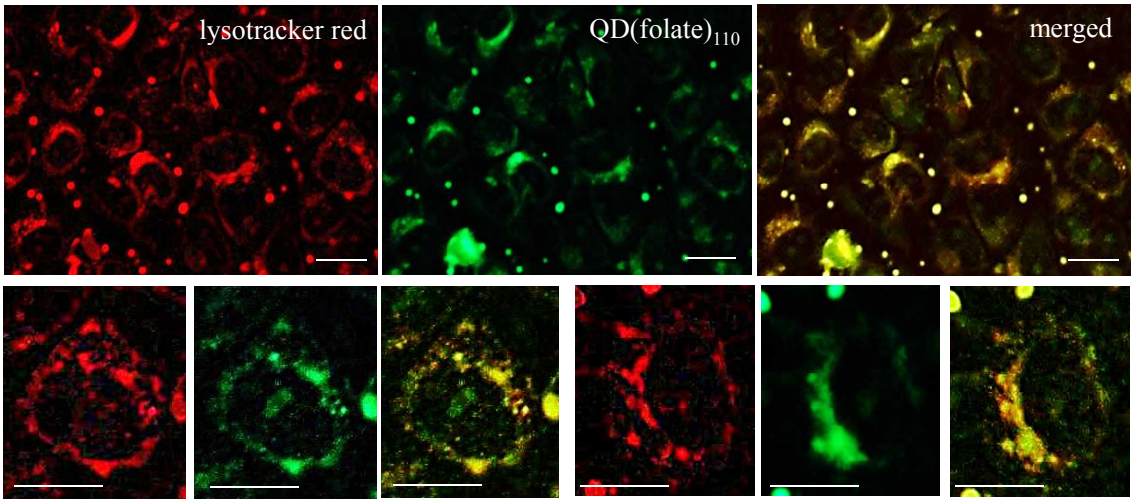

Figure 6. Low and high magnification fluorescence image of QD(folate)$_{110}$ and lysotraker labelled HeLa cells. Here cells are incubated with sample for 3 hrs and washed cells are further treated with media for next 12 hrs for imaging. Red color corresponds to lysotracker, green color corresponds to QD and yellow color in merged image indicates the colocalization. Scale bar represents 20 μm.

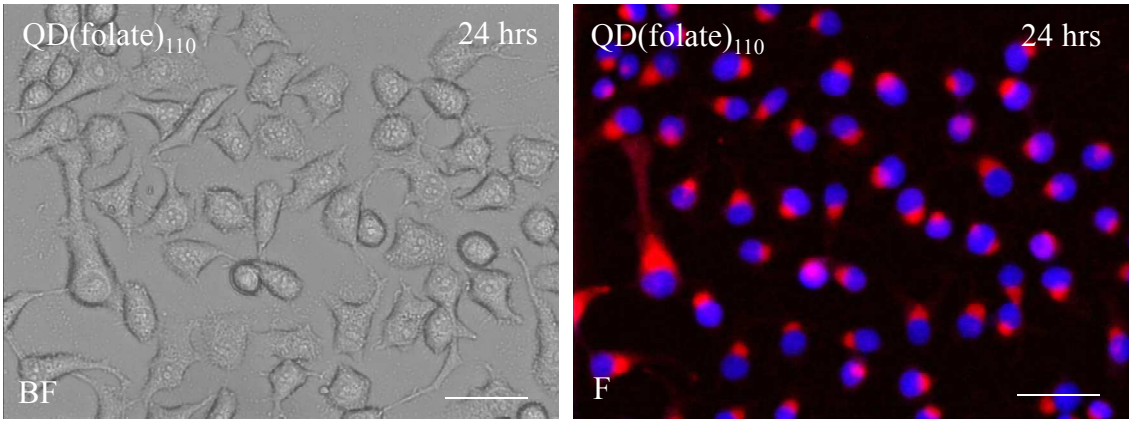

Figure 7. Change in subcellular localization of QD(folate)$_{110}$ in presence of CHP inhibitor. KB cell is first incubated with CHP followed by incubation with QD(folate)$_{110}$ and washed cells are mixed with fresh culture medium for another 24 hrs before imaging under bright field (BF) or fluorescence (F) mode. Red color corresponds to QD and blue color corresponds to nuclear probe. Merged fluorescence image indicates perinuclear localization of QD(folate)$_{110}$. Scale bar represents 50 μm.

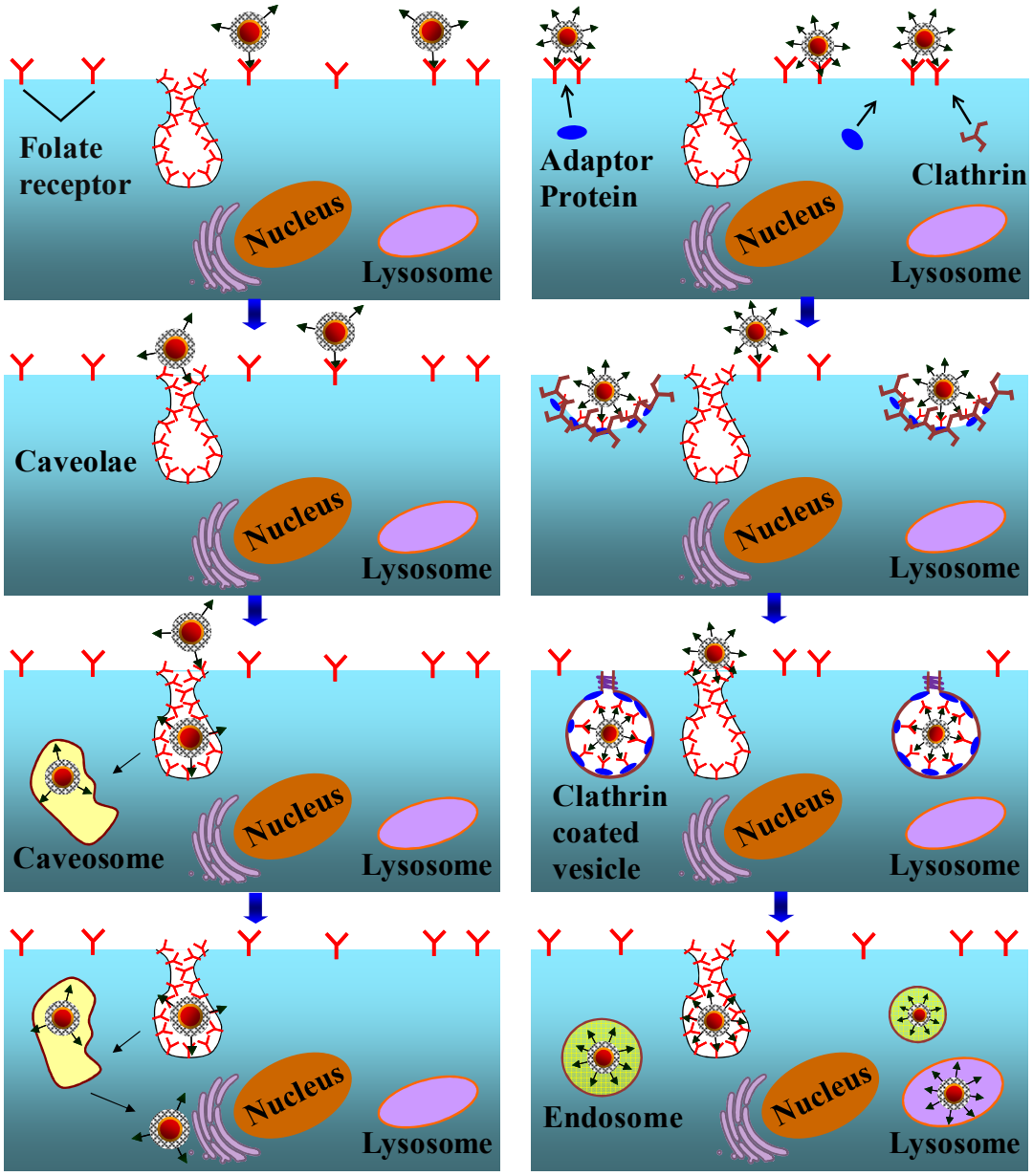

Scheme 2. Proposed endocytosis mechanism of nanoprobe with low and high multivalency. Low multivalency offers modular interaction with cell surface receptors that directs the nanoprobe toward caveolae and promotes caveolae-mediated endocytosis. In contrast, high multivalency offers strong binding of nanoprobe with cell surface via multiple receptors and induce signaling pathway for clathrin-mediated rapid endocytosis.

TOC IMAGE

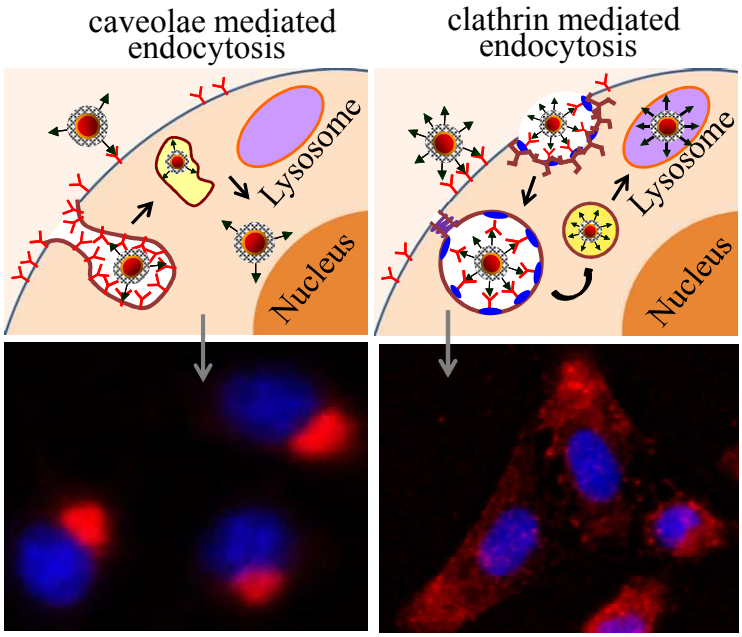

blue- nuclear probe, red- nanoprobe